Optimal Use of Radar Radial Winds in the HARMONIE Numerical Weather Prediction System

MARTIN RIDAL,[a] JANA SANCHEZ-ARRIOLA,[b] AND MATS DAHLBOM[c]

[a] *Swedish Meteorological and Hydrological Institute, Norrkoping, Sweden*
[b] *Agencia Estatal de Meteorologia, Santander, Spain*
[c] *Danish Meteorological Institute, Copenhagen, Denmark*

(Manuscript received 26 January 2023, in final form 21 September 2023, accepted 5 October 2023)

ABSTRACT: The use of radial velocity information from the European weather radar network is a challenging task, because of a heterogeneous radar network and the different ways of providing the Doppler velocity information. Preprocessing is therefore needed to harmonize the data. Radar observations consist of a very high resolution dataset, which means that it is both demanding to process as well as that the inherent resolution is much higher than the model resolution. One way of reducing the number of data is to create "super observations" (SO) by averaging observations in a predefined area. This paper describes the preprocessing necessary to use radar radial velocities in the data assimilation where the SO construction is included. Our main focus is to optimize the use of radial velocities in the HARMONIE–AROME numerical weather model. Several experiments were run to find the best settings for first-guess check limits as well as a tuning of the observation error value. The optimal size of the SO and the corresponding thinning distance for radar radial velocities was also studied. It was found that the radial velocity information and the reflectivity from weather radars can be treated differently when it comes to the size of the SO and the thinning. A positive impact was found when adding the velocities together with the reflectivity using the same SO size and thinning distance, but the best results were found when the SO and thinning distance for the radial velocities are smaller than the corresponding values for reflectivity.

KEYWORDS: Radars/radar observations; Numerical weather prediction/forecasting; Data assimilation

1. Introduction

The aim of this paper is to report the effort and progress made to use of radial velocity data (on top of that of reflectivity) from a large section of radars from the European weather radar network and to show the results of solid improvement of the forecast skill in the limited-area regime. Furthermore, this paper describes the process to find the optimal settings for the radar radial velocity assimilation as well as the performance of impact experiments to verify the optimizations against a reference experiment.

The need for accurate forecasts of high impact weather increases as it is expected that weather events such as intense precipitation will increase, both in frequency and intensity, in the near future. To minimize the expected impact and hence cost to the society, more accurate numerical weather prediction (NWP) forecasts are therefore of great importance. The current trend of steadily increasing model resolution also highlights the importance of using high-resolution datasets in an optimal way. Ground-based weather radars provide such high-resolution datasets, both spatially and temporally. Weather radars give a three-dimensional observation of precipitation intensity, while simultaneously providing a measure of the movement of the precipitation, and thereby an observation of the radial velocity. The latter is derived from the Doppler shift in the transmitted signal relative to the received signal.

The radar observations in Europe are coordinated through the European Meteorological Network (EUMETNET) program Operational Programme for the Exchange of Weather Radar Information (OPERA; Huuskonen et al. 2014). Through OPERA radar observations from most countries in Europe can be obtained and used for NWP purposes as well as other applications. The radar data used in this study have been collected, processed, quality controlled, and redistributed by OPERA. The radar stations in Europe form a heterogeneous network, as the individual member states own and operate them autonomously and hence the scanning strategies are based on nationals needs and requirements. Most countries in Europe operate radar networks containing multiple radar stations providing a very dense observational coverage on a subhourly scale of said country. The OPERA program requires from the national members that they send reflectivity data along with all essential properties of those data in a specific format, the OPERA Data Information Model (ODIM), whereas so far it has only been encouraged that also the radial velocity data are included. However, as long as the data are following the ODIM format, each country can send in full volumes, parts of thereof or even multiple single scans that OPERA then attempts to merge. This along with the varying scanning strategies means that the resulting volume files are heterogeneous.

Various approaches to make use of Doppler radar radial velocity observations in NWP models have been developed during the years, for example, in the Weather Research and Forecasting (WRF) Modeling system (Sun 2005), the High-Resolution Limited-Area Model (HIRLAM; Salonen et al. 2008, 2009) or

Denotes content that is immediately available upon publication as open access.

Corresponding author: Martin Ridal, martin.ridal@smhi.se

DOI: 10.1175/JAMC-D-23-0013.1

the Fifth-generation Pennsylvania State University–NCAR Mesoscale Model (MM5; Xiao et al. 2005). Simonin et al. (2014) developed further the work by Rihan et al. (2008) at the Met Office.

Assimilation of radial velocity has also shown a positive impact on precipitation forecasts using the Applications of Research to Operations at Mesoscale (AROME) model system at Météo-France. The observations operators developed for AROME by Montmerle and Faccani (2009) are used in the system HIRLAM Aire Limitée Adaptation Dynamique Développement International (ALADIN) Research Mesoscale Operational NWP In Europe (HARMONIE; Bengtsson et al. 2017)

The NWP HARMONIE–AROME system was adapted for the use of radar observations from OPERA (Caumont et al. 2010; Ridal and Dahlbom 2017) and reflectivity is currently used by several countries in operations. Radial velocity, however, is only used operationally by Meteorological Co-operation on Operational (MetCoOp), Météo-France (Montmerle and Faccani 2009), and Met Office (Simonin et al. 2014), but it is being monitored by several other institutes in preoperational setups. MetCoOp is the operational cooperation between Norway, Sweden, Finland, and Estonia (Müller et al. 2017).

The experiments in this study are run over the MetCoOp domain using the HARMONIE–AROME system with a horizontal resolution of 2.5 km and 65 vertical levels. The domain, 960 × 1080 grid points, is displayed in Fig. 1. For the upper-air analysis conventional observations are included as well as satellite radiance from several instruments, radar reflectivity, scatterometer data, and ground-based Global Navigation Satellite System (GNSS)–derived observations.

The high-resolution nature of the radar observations implies that the vast number of observations needs to be reduced prior to being ingested into and used beneficially by the data assimilation system in the NWP model. There are several reasons why this is of crucial importance, for example, to avoid possible spatial correlations and representativeness errors as well as avoiding memory issues during the data assimilation. The radar data are commonly being exchanged with a resolution on the scale of hundreds of meters while NWP models typically operate in the km scale, and in the presented study the resolution is 2.5 km. The data reduction can be made in various ways and for radar observations in the HARMONIE–AROME system, "super observation" (SO) construction has been chosen as described in Ridal and Dahlbom (2017). SO is a well-known concept and has been used previously in similar situations to handle various observational data (Benjamin 1989; Simonin et al. 2019). This approach was also proven to be beneficial already when using radar observations in the old HIRLAM system (Lindskog et al. 2000, 2004).

Earlier attempts of assimilating radar velocity observations in HARMONIE–AROME showed poor results and the reasons for these results are investigated in detail in this study. Apart from a few radar stations that provided poor quality radial velocities, prompting the need for additional quality control of individual radar stations, a few settings in the data assimilation system, like the first-guess check limit and observations error, were also found to be suboptimal. Therefore, to include radial velocity information, a further development of the preprocessing and an investigation of the optimal use of OPERA data has been performed.

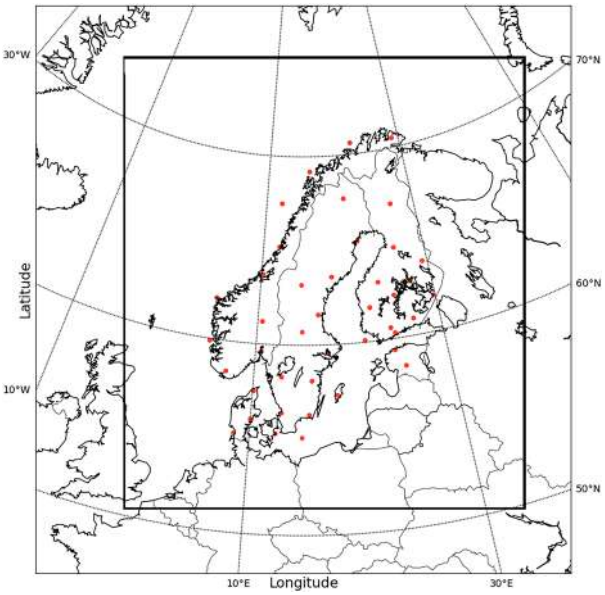

FIG. 1. The MetCoOp operational model domain and the domain used in the experiments in this study. The locations of the included radar stations are indicated by the red dots.

The outline of this paper is as follows: In section 2, the OPERA radar data are described, followed by a description of the SO construction in section 3, and the optimal settings for radar velocities in section 4. The experiments performed are described in section 5, and the discussion and results are presented in section 6. In section 7, some selected cases are studied, and some conclusions are in section 8.

2. Radar data

For this study, volume data from the OPERA network has been used covering the MetCoOp domain. This includes about 42 radars from five countries as indicated by the red dots in Fig. 1. For reflectivity, a few radars in northern Germany are also included but these do not provide any radial velocities and are therefore not included in Fig. 1.

The OPERA data comes in a standardized format and the reflectivity observations are quality controlled before they are disseminated. The quality control (QC) is made by OPERA using the "Bropo package" (Michelson and Henja 2012). The Bropo quality control includes several filters like detection of land and sea clutter, and detection of nonprecipitation echoes (birds, insects, etc.), ships and wireless communication disturbances. All radars are quality controlled using the same settings with a few exceptions. Another feature is that not all OPERA quality methods are applied to all radars. This depends on where the radar is located and the surrounding area. In addition, a beam blockage map is included for each radar resulting in that any echoes from the blocked areas are either removed or filled in if the blockage is only partial. The result

from the quality control is a quality index for each observation point stating the probability of anomaly. Provided with the quality index, it is then up to the user to decide upon a threshold value of the probability that would lead to accepting or disregarding the data.

Even though the radar data obtained from OPERA follow a standard file format, there are differences in the data between different data providers or countries. One example is the scanning strategy. The scanning with a Doppler weather radar can be optimized for either reflectivity observations or for radial velocity observations. A radial velocity optimized scan, or volume, would imply both a higher Nyquist velocity and, as a consequence, a shorter maximum distance from the radar, than that of a reflectivity optimized scan.

The scan strategy in OPERA data differs between different countries, and the reporting practice differs very much. While some countries provide radar volumes where every second volume is optimized for reflectivity and radial velocity, respectively, other countries provide a mix of radial velocity and reflectivity optimized scans in one volume or some sort of compromise between the two. These differences imply a challenge for the users to select the correct observations for the intended purpose without compromising the usability nor the quality of the resulting observations.

In addition to the OPERA data, radial velocity optimized scans from Norway are available for the MetCoOp domain through a bilateral observation exchange. The reflectivity from this dataset is quality controlled slightly differently than that of OPERA (C. Elo 2018, personal communication), but the quality index follows the OPERA standard and hence can be used in exactly the same way as the ones produced by OPERA.

Due to this diversity in the data, a preprocessing step is necessary before the radar observations can be used in the data assimilation. In HARMONIE–AROME a preprocessing script has been developed to harmonize the observations when it comes to observation density and to check that all necessary metadata is available and of the correct units. If something is missing, the correct value is added if known, or else that radar or scan will be disregarded. The preprocessing is described in detail by Ridal and Dahlbom (2017).

For the data assimilation, the radar reflectivity is not directly assimilated since there is a complicated, nonlinear relation between the model variables and reflectivity. This includes parameterizations of microphysical processes and non-Gaussian error distributions. Instead, a vertical moisture profile is retrieved through a one-dimensional (1D) Bayesian retrieval based on a comparison between observed and simulated reflectivities. This humidity profile is then used in the 3D-Var assimilation scheme. The method is described in detail in Caumont et al. (2010) and Wattrelot et al. (2014).

The radial velocities on the other hand, are used directly in the data assimilation by comparing with a model equivalent calculated for each radar through the observation operator. The observation operator was developed by Montmerle and Faccani (2009), based on Salonen et al. (2008) and Caumont et al. (2006), and takes into account the beamwidth of the radar as well as the bending of the radar beam in order to include the correct model levels.

One complicating factor when assimilating the radial velocities is that the radial velocity itself is not quality controlled by OPERA. There is a first quality control performed by the signal processor at the radar site. However, there is no QC similar to the ones available for reflectivity to remove sea and ground clutter and similar "false" echoes. The solution to this that has been chosen here is to use the quality information for reflectivity and apply this to the radial velocity observations. Therefore, it is necessary that a reflectivity field is provided together with the radial velocity field in the data files. If this is not the case, the radial velocity observations will not be used.

Another effect that complicates the use of radial velocities is that aliasing can occur. Aliasing effects may appear as sudden changes in the velocity strength and direction in which case assimilation of the data would be devastating for the resulting analysis. The Nyquist velocity, or Nyquist interval (NI), is the maximum velocity that the radar can measure without risking the appearance of any aliasing effects. Within the OPERA network the NI can vary from very low to high depending on what the specific scan is optimized for. Although there are dealiasing algorithms available (e.g., Ray and Ziegler 1977; Haase and Landelius 2004; He et al. 2019), in this study, no dealiasing algorithm has been applied. Instead, all observations with a NI value lower than 30 m s^{-1} were disregarded in the preprocessing and not included in the experiments.

3. Super observation construction

The OPERA radar observations compose a high-resolution dataset. To make use of the data in an efficient manner and to avoid memory problems when ingesting the observations to the data assimilation system, a reduction of the data amount is necessary. This is done in the preprocessing step described in the previous section together with the harmonization of the data.

There are several methods to perform a data reduction. In this study, construction of SO (Purser et al. 2000) was chosen to reduce the number of data but still keep as much information as possible. Since SO also makes an average over an area, it is an efficient way to sort out outliers. This is especially important for radar radial velocities since the wind direction sometimes can change rapidly, for example, during a frontal passage and strong convection episodes. It can also be an indication that aliasing effects exist. The internal variability of the SO is therefore checked before accepting the final SO to make sure that the standard deviation is below some user defined limit. In this study the standard deviation of the SO must be below 5 m s^{-1}.

Since there is averaging involved, the size of the SO is important (Frehlich 2008). If the size is too large, there is a risk of losing important information like very high wind speeds. The internal variability will also be higher, so more observations will be lost because of its limit. It is therefore of interest to keep the SO as small as possible but still large enough to sufficiently reduce the data.

For each elevation angle, the radar measures in a grid around the radar in bins away from the radar and azimuth angles in the circular sweep. The original resolution of this grid

can be very different depending on the data producer, but it can also vary for different elevation angles within volume. During the SO construction, a new grid size is determined. To account for the diverse input the new grid spacing is given in meters for the range distance and in degrees for azimuth direction instead of a fixed number of bins or azimuth gates. That will ensure a homogeneous output regardless of the input data. Since this is done for each elevation angle separately the method is also independent of the number of elevation angles for each radar.

All observations within the new grid are stepped through to examine the observed value and the quality information. If the observation value is reasonable and of acceptable quality, the observation is included in the SO. The result will be SOs consisting solely of observations of good quality. If the majority of the observations indicate precipitation, it will be an observation of precipitation and if the majority are clear sky observation it will be classified as a dry observation. Dry observations are important so as to remove precipitation in the first-guess field that is placed in the wrong location. If there are too few observations accepted within the SO, it will be disregarded and classified as a nonexistent observation. The creation of the SOs as well as a comparison with a simple data thinning is described in detail in Ridal and Dahlbom (2017).

The quality information is crucial for the SO construction and currently, there is no quality information available for radial velocity in the OPERA data. Therefore, to have some control over the quality of the observations, the quality index for reflectivity is used also in the construction of the SO for radial velocities. It is therefore important that all volumes and scans that contain radial velocity information also contain the corresponding reflectivity field. Unfortunately, this is not the case for all data providers, and in these cases the radial velocity information cannot be used and the scan will be disregarded. The quality index is available for all reflectivity fields even if the scan is optimized for radial velocity observations.

4. Optimized radial velocity usage

In the first attempts to include the radial velocities from radars the results were not satisfactory. During the following investigations of possible reasons a few issues were identified as nonoptimal in the data assimilation, all of them allowing bad quality data to enter the data assimilation. These issues and the solutions adopted are described below.

a. *First-guess check*

The first-guess check step in the process of including an observation in the data assimilation is what controls that the observations are not too different than the first guess, or model background field. The first guess is normally a short-range forecast, in this study it is a 3-h forecast. If the observations are found to be very different from the model equivalent, the observation will be disregarded.

To investigate the first-guess check limits the Anderson and Järvinen (1999) technique was followed to examine the histograms and inverse histograms of background and analysis departures. This was done for an experiment that assimilated, apart from conventional and satellite observations, radar radial velocity with the default settings prior to this study. In the case of radar radial velocity, it was found that the first-guess check limit set by default was too generous in HARMONIE–AROME. The histograms in Fig. 2 show the first-guess departures for radar velocity from this experiment. Figure 2 (left) shows the so-called transformed histogram of observation departures for the background that have been transformed according to

$$f = \sqrt{-2 \ln\left[\frac{f}{\max(f)}\right]}, \tag{1}$$

where f is the number of data in each bin of the histogram (Hollingsworth 1989). The slope of the points, indicated by red lines, defines the standard deviation of the Gaussian curve that is represented in Fig. 2 (right). The rejection limit is set some distance beyond the point where f crosses start to be separated from the straight lines. It is seen in Fig. 2 (right) that out to ±5–6 m s^{-1} the first-guess departures show a Gaussian behavior while for the higher values they form tails (noncompliant to a Gaussian distribution). This is believed to be one reason why the impact on the forecasts of the assimilation of radial velocity was detrimental. As a result of this, a new first-guess check limit of 5 m s^{-1} instead of 20 m s^{-1}, default in HARMONIE–AROME, was set for the next experiments.

b. *Observation error*

Another step to make an extensive diagnosis of the assimilation of the radial velocity was to find out the optimal observation error value for the radial velocities. The first step was to compare it with other wind observations such as aircraft or radiosondes. It was discovered, as illustrated in Fig. 3 (left), that the previously used value was set to be lower, around 1.5 m s^{-1} (denoted as "radar" with red markers), than the values used for both aircraft wind observations (blue) and radiosonde winds (green). The reason it is more spread out relative to the observation error for radiosondes and aircraft observations is that the observation error value for radar radial velocity increases with distance from the radar.

This lower value of observation error implied that the radar radial velocities had much more weight in the analysis when compared with the other wind observations. A consequence of giving one observation too much weight, often referred to as overfitting, can result in imbalances in the model system. In such cases, even though the analysis looks good, problems can occur once the forecast run starts. Figure 3 (right) shows a new and more conservative observation error value chosen for radar radial velocities, that would be around 2.5 m s^{-1}. This average value was selected after having performed several experiments prior to this study where a number of different observation errors were tested.

After having increased the observation error for radar radial velocity, one way of visualizing the relative impact of each observation in the data assimilation is to use the degrees of freedom for signal (DFS; Chapnik et al. 2006). DFS is the derivative of the analysis increments in observation space

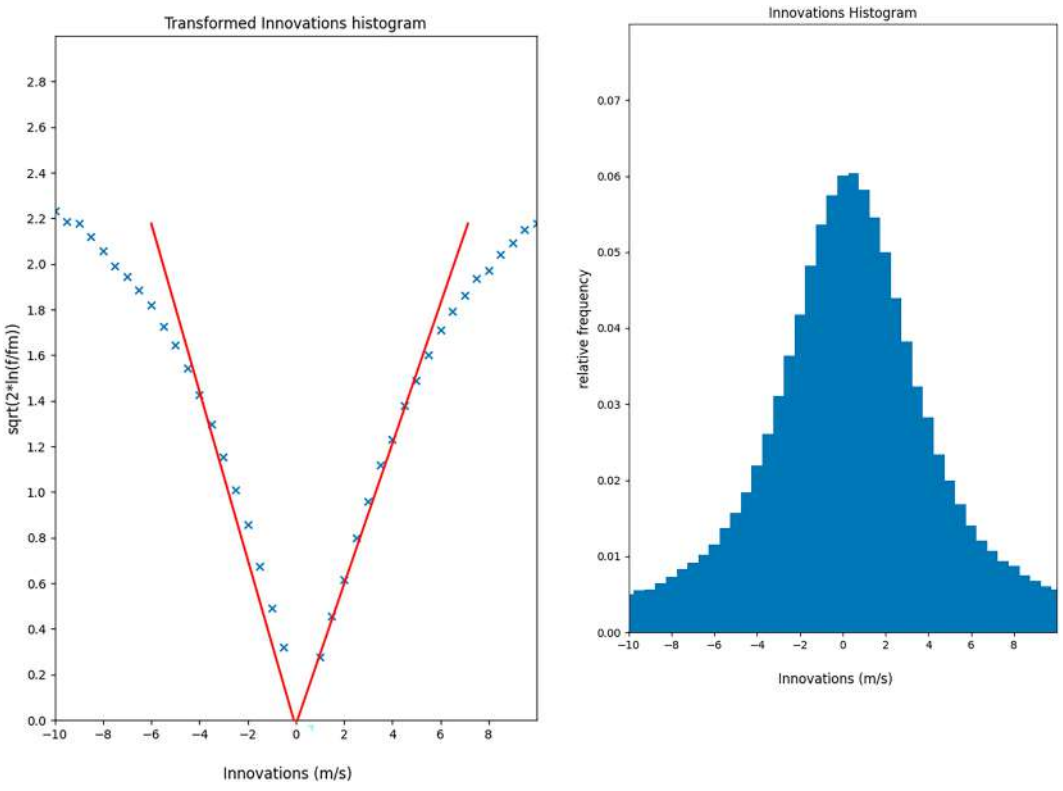

FIG. 2. (left) Transformed histogram and (right) histogram of the first-guess departures of radial velocities.

with respect to the observations used in the analysis system. The DFS statistics offer an insight to the actual weight given to the observations within the analysis system in terms of self-sensitivity of the observations (i.e., sensitivity at observation location).

As proposed by Chapnik et al. (2006), DFS can be computed through a randomization technique:

$$\mathrm{DFS} = \frac{\partial H x_b}{\partial y} \approx (\tilde{\mathbf{y}} - \mathbf{y})\mathbf{R}^{-1}[H(\widetilde{x_a} - x_b) - H(x_a - x_b)], \quad (2)$$

where $\mathbf{y}$ is the vector of the observations; $\tilde{\mathbf{y}}$ is the vector of perturbed observations: $\mathbf{R}$ is the observation-error covariance matrix; H is the tangent-linear observation operator for each observation type; x_a and x_b are the analysis and the background state, respectively; and $\widetilde{x_a}$ is the analysis produced with perturbed observations. The formulation can be applied to any subset of observations (Randriamampianina et al. 2011).

In Fig. 4, DFS statistics for an experiment using a too-low observation error for radar radial velocities is shown in Fig. 4 (left panel), together with the same statistics from an experiment using a more suitable observation error in Fig. 4 (right panel). It is clearly seen that with too-low observation error the radar radial velocities (RADAR DOW) are weighted much higher than any other observation. However, with the higher observation error, the weight is much more similar to the other wind observations from radiosondes (TEMP U) and aircraft (AIREP U).

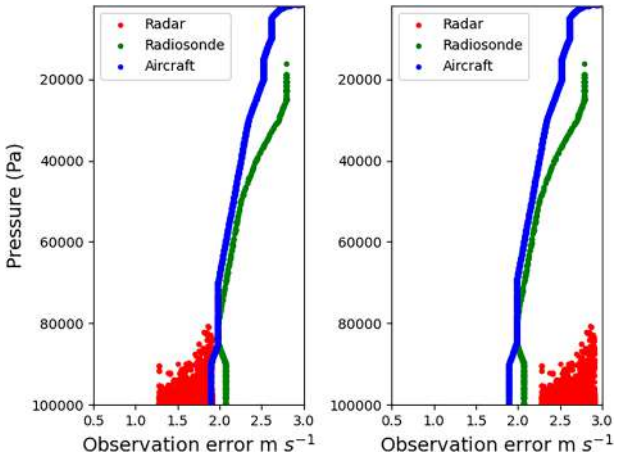

FIG. 3. Value of the observation error for radar radial velocity (red dots), aircraft wind (blue dots), and radiosonde wind (green dots) (left) before and (right) after increasing the observation error for the radar radial velocity.

c. *Thinning distance*

Observations measured from the same platform often come with correlated errors if part of the observation error is due to the instrument or the placement of the instrument (Simonin et al. 2019). The correlations can occur in both space and time

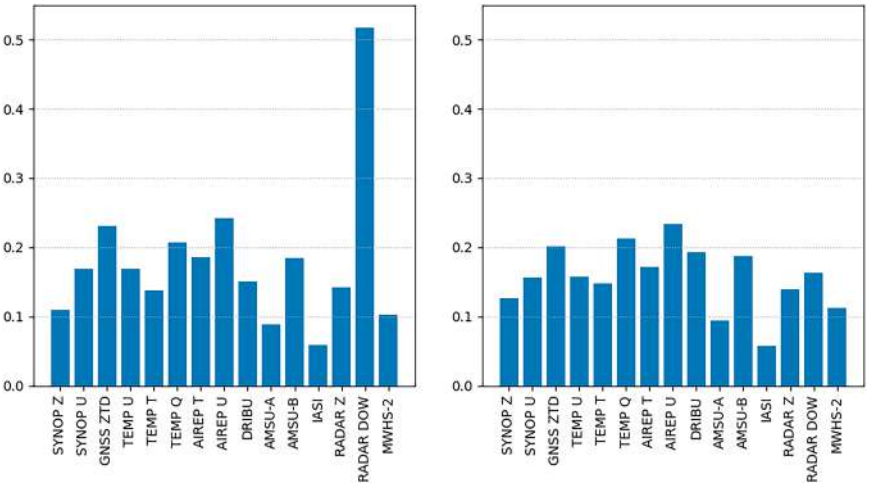

FIG. 4. Relative DFS for (left) a case with low observation error for radar radial velocity (RADAR DOW) and (right) a case with adjusted, more suitable, observation error for radar radial velocity.

and since there is not a proper way to handle this kind of errors in the current data assimilation system the best solution is to try to avoid them. In a 3Dvar assimilation system, nonmoving observations are used only once every 3 h. This means that there are basically no temporal correlations that need to be addressed. The spatial correlations, however, need to be avoided somehow. The easiest way is by reducing the number of data in the data assimilation, usually referred to as data thinning. In the case of radar observations, this thinning is different from the one that is performed in the preprocessing where the SOs are constructed. The thinning in the data assimilation is the final horizontal resolution of observations used, decided from different criteria.

For radar data, the thinning in the data assimilation is designed to choose observations in a way that they will not be located closer to each other than some given limit. The final thinning distance in the data assimilation depends on the NWP model resolution and the type of observation (Bormann and Bauer 2010).

According to Desroziers method (Desroziers et al. 2005) the thinning distances used for radar radial velocities SOs for this study were too short. In Fig. 5 it can be seen how the spatial error correlations between different SOs changes with the distance between two SOs. As seen in this figure, the distance between two radial velocity SOs to have spatial error correlation close to zero should be about 60 km. Such a long thinning distance would lead to rejecting a lot of good radar SOs so in this study it was chosen to start with a thinning distance of 15 km. This would imply having a spatial error correlation of about 0.20, which is considered to be low enough for data assimilation (Liu and Rabier 2003).

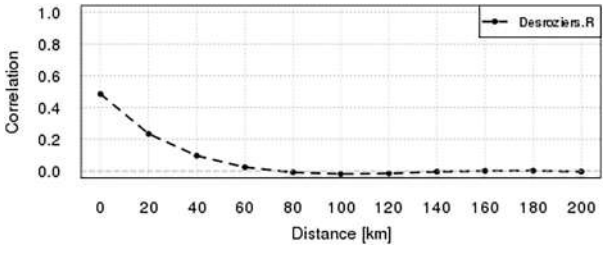

FIG. 5. Spatial error correlation according to the distance between two radial velocity super observations derived using the Desroziers method.

An alternative to decreasing the number of data to handle spatially correlated errors as well as possible representativeness error could instead be to keep the same number of observations but increase the observation error. It is even possible to increase the number of observations using this approach and thereby introduce small-scale observations to the data assimilation but with less weight. Good results using this method have been shown for other observation types like lidar wind observations from satellite by the Aeolus instrument (Rennie et al. 2021; Hagelin et al. 2021) or surface pressure observations collected from smart phones in Denmark (K. Hintz 2022, personal communication) and it was therefore tried in this study.

5. Experiments

After some previous tests to decide the settings described in the previous section, several experiments were run for a 3-week period in August 2021. All experiments run using the Meteorological Co-operation on Operational (MetCoOp) NWP operational model set up and domain. Inside the model domain there are 45 radars from six countries that are included in the daily production. During the chosen period, several large-scale frontal systems passed through the model domain and also a few convective situations occurred.

The reference experiment was run with an additional 2-week spinup period to get all of the fields in balance and to allow the variational bias correction coefficients to spin up properly. All

TABLE 1. Summary of the experiments. The SOs are created in a preprocessing step, and the number indicates the radius of the SO. The final thinning is decided in the data assimilation procedure, and the number indicates the distance between observations used in the minimization.

Expt	Reflectivity SO size (km)	Reflectivity thinning (km)	Radial velocity SO size (km)	Radial velocity thinning (km)	Obs error (m s^{-1})
Reference	6	15	—	—	—
Exp1	6	15	6	15	2.5
Exp2	6	15	3	15	2.5
Exp3	6	15	3	7.5	4

the other experiments in this study were also warm started from this spinup period.

The experiments are run with a 3-h cycling with forecast up to 24-h lead time at 0000, 0600, 1200, and 1800 UTC. During the intermediate hours, only the 3-h forecasts are produced that serve as first guess in the following analysis. The experiments include all the observations used in the MetCoOp operational runs, that is, conventional observations [synoptic (synop) stations, ships, aircraft including mode-selective enhanced surveillance (Mode-S) data and radio soundings], satellite radiances from the Advanced Microwave Sounding Unit (AMSU)-A, the Microwave Humidity Sounder (MHS) and the Infrared Atmospheric Sounding Interferometer (IASI), scatterometer winds, ground-based Global Navigational Satellite System (GNSS) and radar reflectivity.

The two filters for radar radial velocity described in the previous section were applied to all the radial velocity experiments, that is, tighter first-guess check limit and higher observation error. All experiments are run with the same settings for reflectivity as in the operational runs, that is, 6 km SO and a thinning of 15 km for the active observations. Attempts were made to decrease the thinning for reflectivity, but the results were not satisfactory, so these experiments were not further explored.

Four experiments were included in this study. One of these is the reference experiment that is similar to the operational MetCoOp run, while the other three experiments used different settings for the assimilation of radar radial velocity to investigate the optimal use of these observations.

A more detail description of the experiments is as follows: In the reference experiment, no radar radial velocity observations are included. It has the same setup as the MetCoOp operational runs. Radar reflectivities are included using a SO size of 6 km in bin size and 3° in azimuth direction. The final thinning in the data assimilation step for reflectivity is 15 km.

In experiment 1 (Exp1), radar radial velocity observations are included with 6-km, 3° SO, and equal thinning for both radial velocities and reflectivities (15 km). In this first experiment, the radial velocities were added with the same size of SO as reflectivity when used in the reference run, 6 km and 3° azimuth angles, and with the same thinning as in the reference experiment (15 km). Therefore, in this case the same SO size and thinning in the data assimilation is used for both reflectivity and radial velocity.

In experiment 2 (Exp2), radar radial velocity observations are included with 3-km, 2° SO, and equal thinning for both radial velocities and reflectivities (15 km). In an attempt to increase the small-scale information, the size of the SO was decreased to about one-half of the size. The thinning in the data assimilation, however, was still the same. This means that radial velocity and reflectivity were used differently in the assimilation.

The drawback with this approach is that the preprocessing needs to be run two times: once for reflectivity and once for radial velocity. It also means that the number of data is more than doubled since the data assimilation is designed so that arrays for both reflectivity and radial velocity are allocated even

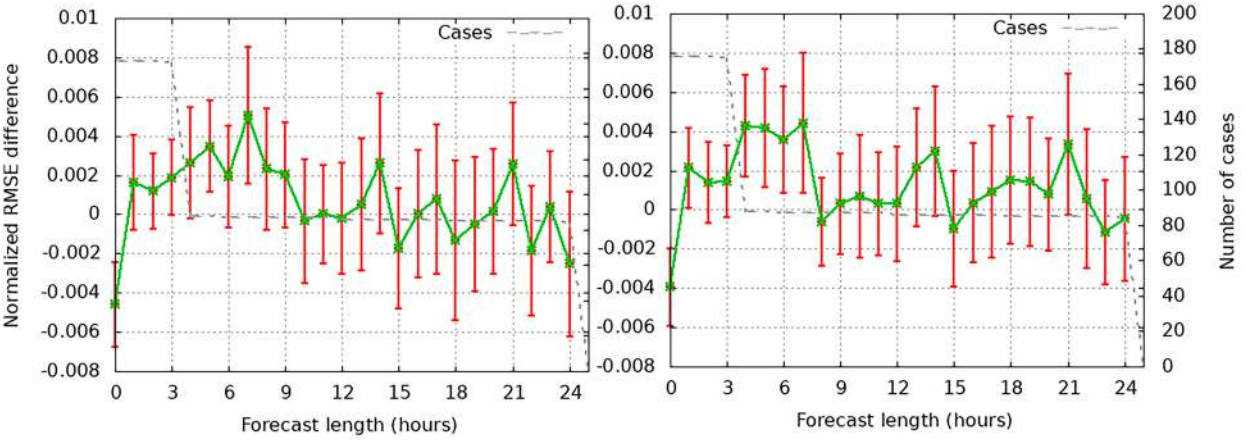

FIG. 6. Significance test of normalized RMSE for wind speed at 10 m for (left) Exp1 in comparison with the reference experiment and (right) Exp3 in comparison with the reference experiment. Positive values mean smaller RMSE for the radial velocity experiments and thus a positive impact on the forecasts. The number of cases refers to the number of verification times.

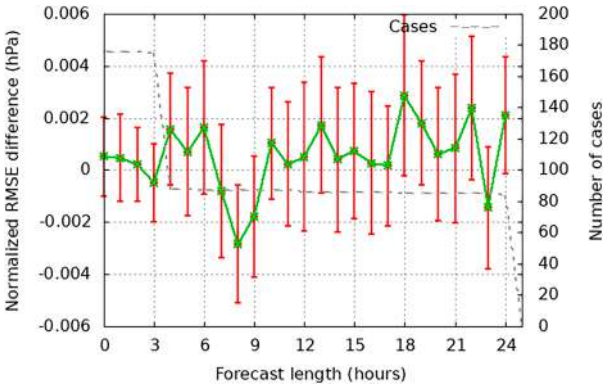

FIG. 7. Significance test of normalized RMSE for wind speed at 10 m for Exp3 in comparison with Exp1. Positive values mean smaller RMSE for Exp3 and thus a positive impact on the forecasts. The number of cases refers to the number of verification times.

though just one will be used. Note that reflectivity is still needed to accompany the radial velocity observations so as to use the quality information even though it is not used in the assimilation.

The advantage with this approach is that reflectivity and radial velocity will be independent and can be taken from different scans of the radar. Reflectivity can be used from reflectivity optimized scans while the radial velocity information can be taken from radial velocity optimized scans, using a high NI.

For this experiment, about 2–3 times as many humidity observations enter the assimilation system as in the reference experiment even though the ones associated with the radial velocity data will not be used. In the minimization, however, the number of both reflectivity and radial velocity observations are about the same due to the unchanged thinning.

Results from this experiment showed a very promising improvement relative to Exp1. These encouraging results lead to the final experiment described below. In experiment 3 (Exp3), the radar radial velocity observations are included with 3-km, 2° SO, and one-half of the thinning distance for radial velocity as compared with reflectivity.

To try to get as much high-resolution information from the radar radial velocities as possible, a last experiment was performed. This one is the same as Exp2 above, but this time with less thinning (lower thinning distance) in the data assimilation to allow more observations to be used. In this case the thinning of radial velocity was set to half of the previous experiments.

This approach increased the amount of radial velocity observations used in the minimization with about the double due to the shorter thinning distance for radial velocity.

For this experiment, the observation error for the radial velocity observations was increased. The reason for the higher observation error is to take into account any spatially correlated or representativeness errors that may occur due to the shorter thinning distance. Again, a few shorter experiments were run to determine the most reasonable value for the observation error. It was finally set to, on average, 4 m s^{-1}, that is, almost double relative to Exp1.

All the experiments and their differences when it comes to thinning and SO size of radar reflectivity and radial velocity handling are summarized in Table 1.

6. Results

The main conclusion obtained after seeing all the results is that adding radar radial velocities on top of the observations used in the reference experiment generally shows improved results.

For most parameters, only results from experiments Exp1 and Exp3 are presented. Exp1 is interesting since the configuration is very similar to what is run operationally using only reflectivity. The radar radial velocity from the same input data files can readily be added and assimilated operationally. A period of monitoring is, however, necessary in order to identify radar stations that need blacklisting due to quality issues. For the domain and period chosen in this study, results from Exp2 and Exp3 are a bit better than from Exp1 and despite both of them being quite similar, Exp3 shows better results in general. An example is shown below for cloud cover.

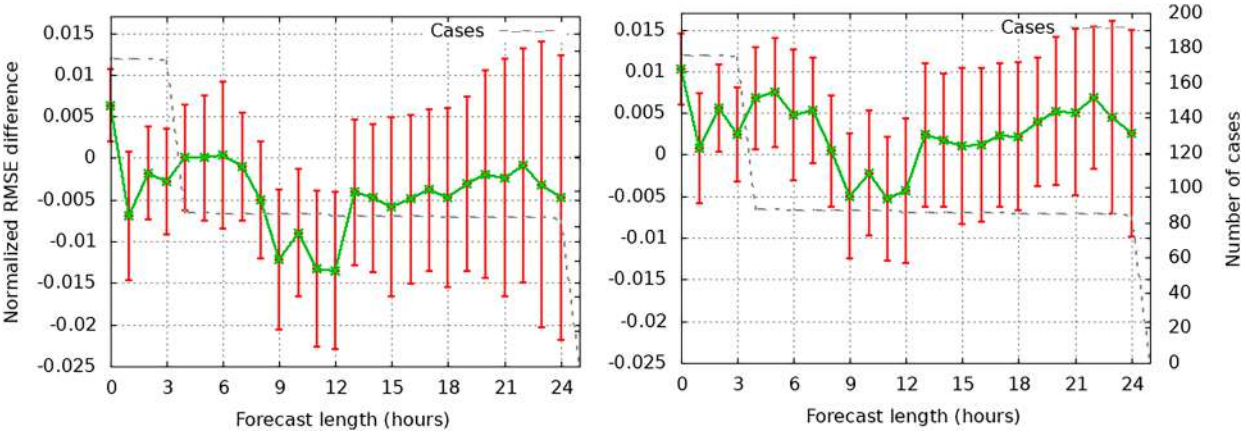

FIG. 8. As in Fig. 6, but for mean sea level pressure.

Results will be explained according to different model variables where the impact of the assimilation of radar radial velocity has been explored. The variables explored are wind speed at 10-m altitude, mean sea level pressure, and temperature and humidity, both at 2-m altitude. These variables are chosen since these are basically the control variables of the model although wind speed is represented by vorticity and divergence in the control variable. If these parameters show good results, it will be beneficial to the entire model system. Cloud cover is also shown since this often is a complicated variable that is important to get correct.

The results in sections 6a–d are presented as the normalized root-mean-square error (RMSE) between observations and model output. The RMSE is defined as

$$\mathrm{RMSE} = \sqrt{\frac{\sum_{n=1}^{N} [x(n) - y(n)]^2}{N}}, \tag{3}$$

where N is the total number of comparisons n, x is the observed value, and y is the corresponding modeled value. The normalization is then performed by dividing by the mean values of the included observations.

The RMSE includes both systematic errors (bias) as well as random errors like standard deviation or mean area error. Both of these types of errors are important in the verification of the NWP results.

a. 10-m wind speed

It is expected that the inclusion of radar radial velocity in the data assimilation will give a positive impact on the 10-m wind speed. And this is the case for all the experiments described above.

Results from verification of Exp1 and Exp3 against observations are presented in Fig. 6. This figure shows a significance test for the normalized root-mean-square error (RMSE) difference relative to the reference experiment, with error bars showing the 90% confidence level as a function of forecast length.

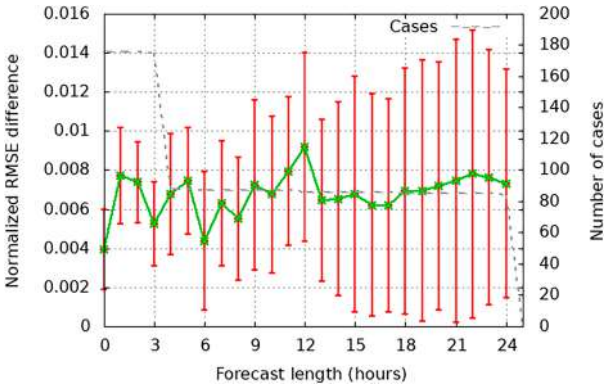

FIG. 9 As in Fig. 7, but for mean sea level pressure.

Although small, a significant improvement can be seen for both cases up to 7–9-h forecast lead times, being more or less neutral afterward when compared with the reference. It can also be seen that Exp3 (Fig. 6, right) shows slightly more positive impact than Exp1 (Fig. 6, left).

In a comparison of Exp1 and Exp3, as shown in Fig. 7, a clear but not significant improvement (except for the 7–9-h forecasts) for Exp3 can be seen, so the extra benefit of decreasing to one-half of the thinning distance for radial velocity is small for this variable.

b. MSLP

In Fig. 8 the mean sea level pressure (MSLP) is presented in the same way as 10 m wind speed in Fig. 6. It can be seen that Exp1 (Fig. 8, left) does not show any positive impact in the MSLP relative to the reference run, whereas a significant positive impact for Exp3 (Fig. 8, right), at least up to 5–7-h forecast lead time, is found relative to the reference.

In Fig. 9, the two experiments including radar radial velocity are compared with each other, and there is a clear, significant positive impact for Exp3 throughout the entire 24-h forecast period. This result means that the reduction of the thinning distance for radial velocity has an impact for MSLP for the first forecast hours.

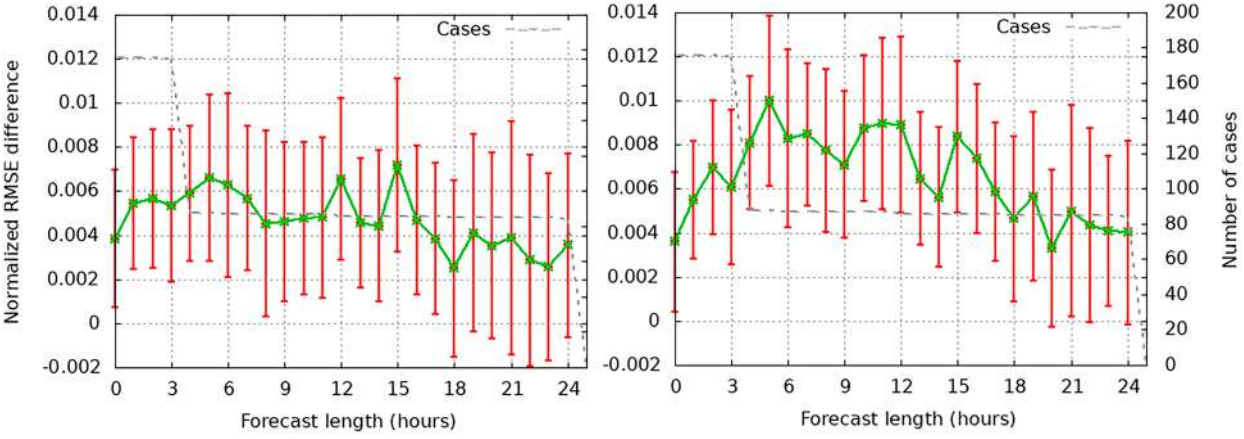

FIG. 10. As in Fig. 6, but for temperature at 2 m.

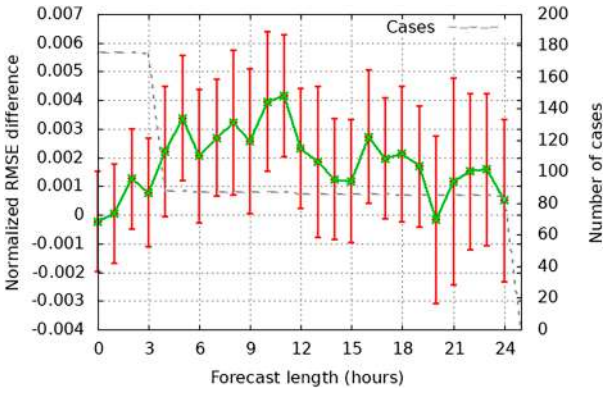

FIG. 11. As in Fig. 7, but for temperature at 2 m.

c. 2-m temperature

What is interesting in the experiments performed here, is that basically all other screen level variables, such as 2-m temperature, benefit from the inclusion of radar radial velocity. This shows that the impact of reflectivity, and possibly other observations, is also increased when the radial velocity is assimilated. To illustrate this, Fig. 10 shows a verification in the same way as in Fig. 6 but for temperature (T2m) at 2-m height.

Both Exp1 and Exp3 show a positive impact from the radial velocity assimilation with a slightly better impact for Exp3 relative to the reference run. In fact, there is a positive impact for T2m throughout the entire 24-h forecast period for the case with higher density radial velocity information (Exp3).

When the two experiments including radial velocities are compared with each other, that is, in comparing Exp1 and Exp3, it can be seen, in Fig. 11, that there is a significant positive impact in Exp3 for forecast ranges of 5–10-h lead time.

d. 2-m relative humidity

The 2-m relative humidity (RH2m) also benefits from adding radial velocity information from the radars. Also, for this variable we see a further improvement for Exp3 relative to Exp1; that is, it benefits from the higher-resolution radial velocity information.

In Fig. 12, the significant tests for RH2m are presented in the same way as in Fig. 6. It can be seen that both cases give a significant improvement, basically throughout the entire 24-h forecasts, when compared with the reference, with an additional benefit in Exp3 (Fig. 12, right).

In comparing the two experiments including radial velocities with each other, that is, Exp1 and Exp3, it can be seen, in Fig. 13, that there is a significant positive impact in Exp3 for forecast ranges up to 6-h lead time.

e. Cloud cover

For the precipitation it is difficult to see any major changes when adding the radial velocity information from radars when verifying the entire period and domain. But one thing that does stand out though is the verification of cloud cover. This is clearly improved when optimizing the use of radar radial velocity.

The Kuiper skill score (KSS) or true skill statistic (TSS) is defined as the probability of detection of an event by the model H minus the false alarm rate F:

$$\mathrm{KSS} = \mathrm{TSS} = H - F = \frac{(ad - bc)}{[(a + c)(b + d)]}, \tag{4}$$

where a is the number of hits in the comparison (observed and forecast), b is the number of false alarms of the model (not observed but forecast), c is the number of misses of the model (observed but not forecast), and d is the number of "nonevents" (not observed and not forecast). Therefore $(a + c)$ is the number of events observed (whether forecast or not forecast), and $(b + d)$ is the number of events not observed (whether forecast or not forecast). The upper limit of the KSS is 1, which represents the perfect forecast (Hanssen and Kuipers 1965). Cloud cover is often described in octas, that is, how many eighths of the sky that are covered by clouds. In Fig. 14, KSS has been plotted for cloud cover forecasts up to 9-h lead time for the different octas of sky covered by clouds for the different experiments. The

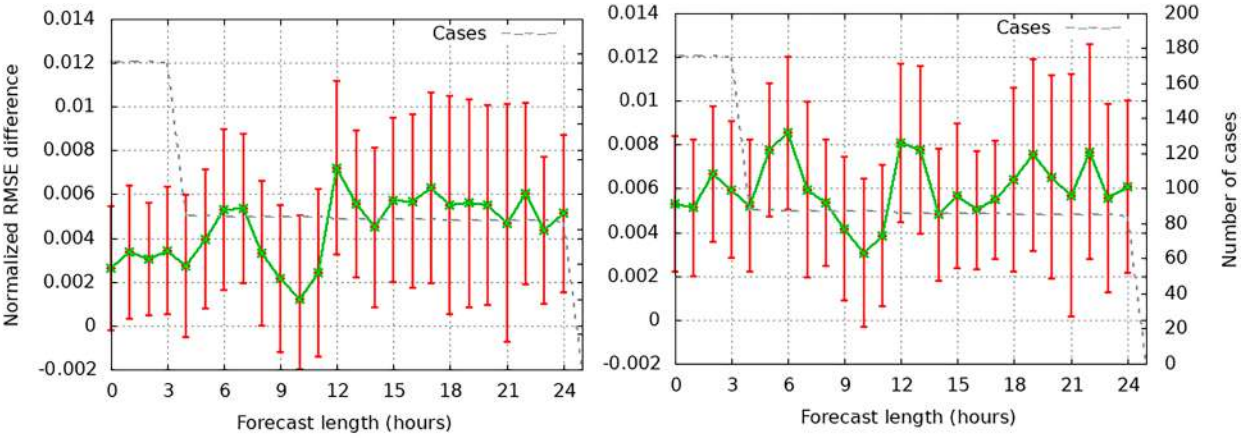

FIG. 12. As in Fig. 6, but for relative humidity at 2 m.

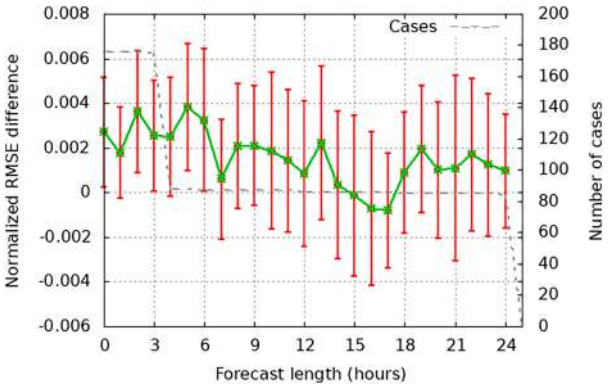

FIG. 13. As in Fig. 7, but for relative humidity at 2 m.

experiments shown are Exp1 (green), Exp2 (blue), Exp3 (purple), and the reference run (red), and it can be seen that the two experiments with smaller size of SO for the radial velocity (Exp2 and Exp3) have a higher KSS and therefore give the best results. A small advantage can be seen for the case with the additional shorter thinning distance (Exp3).

f. Vertical profiles

The vertical profiles for the different variables for the different experiments in comparison with radiosondes show a weakly positive or neutral impact for all variables except for relative and specific humidity. Both humidity variables show a clear positive impact from adding the radial radar velocity but not a clear benefit for the experiments with smaller SO size for radial velocity have been found.

Figure 15 shows the vertical profiles of relative humidity for the reference experiment (red) and Exp1 (green) and Exp3 (blue) verified against radiosondes. At the lowest levels the experiments including radial velocities show better scores (STDV mainly) and at 500 hPa Exp3 shows a clear improvement in STDV too. The reason for the latter is most likely that the radar beam gets very broad at higher altitudes, far away from the radar. A smaller SO would therefore be more beneficial since the covered area will not be unrealistically large.

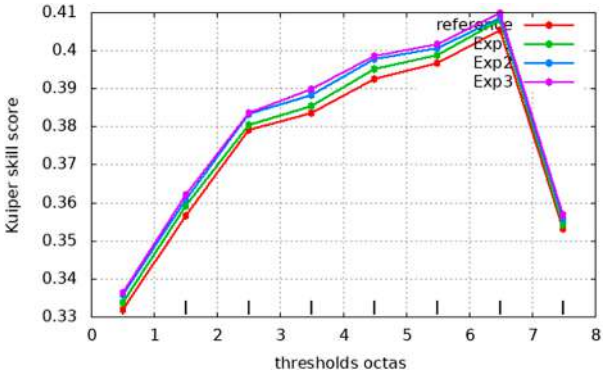

FIG. 14. KSS for cloud cover for the reference experiment (red), Exp1 (green), Exp2 (blue), and Exp3 (purple) against the number of octas of the sky covered by clouds.

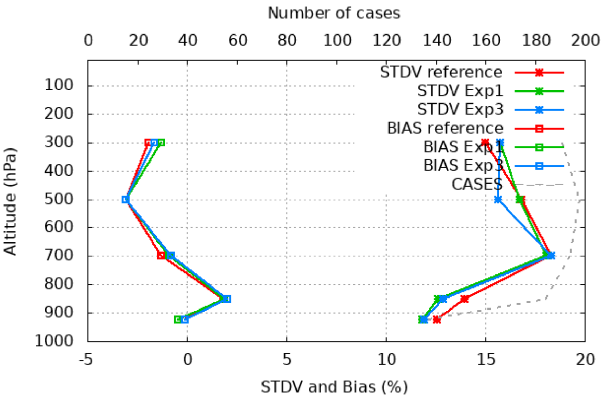

FIG. 15. Verification of vertical profiles of relative humidity for the reference run (red), Exp1 (green), and Exp3 (blue). Squares (left profiles) show the bias, and asterisks (right profiles) show the standard deviation. Number of cases refers to the number of radiosondes in the verification.

7. Case study

Precipitation is difficult to verify in a point verification as presented in the previous section. A small displacement error can show up as a totally wrong forecast. Therefore, verification of precipitation is presented subjectively in a case study.

During the period of 10–31 August 2021, for which the experiments were run, there were two major low pressure systems passing through the domain and many days with lots of convective activity. One interesting thing to examine is if there is any difference in the impact of radar radial velocity in different situations.

In general, the impact on precipitation patterns has been small, which is expected since the added variable is wind related. One fairly clear example was found, however, and is shown below. In addition, by looking at DFS statistics, different behavior could be seen in convective cases than in stratiform cases.

a. DFS statistics

Two examples of DFS diagnostics are presented for two case studies included in the period of study. One from 14 August, in Fig. 16, and the other from 17 August in Fig. 17, both at 1800 UTC.

The 14 August case represents a convective situation while the 17 August case represents a larger-scale frontal passage with more stratiform precipitation. In both cases the number of radar radial velocity observations are about the same and the relative impact of the radar radial velocity seems to be quite similar, that is, no difference in convective or stratiform situations. However, looking at the other observations, it can be seen in the left panels of Figs. 16 and 17 that, without radar radial velocities, the impact of moisture from radiosondes (TEMP-Q) and ground-based GNSS (GNSS-ZTD) are about the same. When the radial velocities are added (right panels of Figs. 16 and 17) on the other hand, the impact from both radiosondes and GNSS changes. Specifically, the impact from

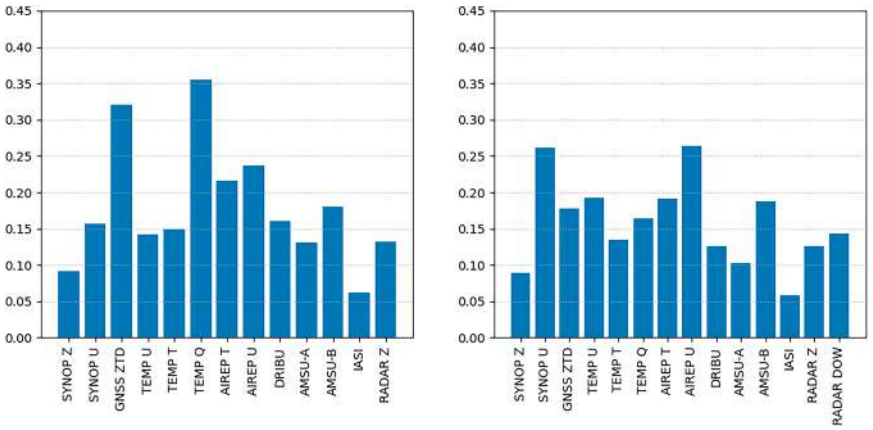

FIG. 16. Relative DFS for the (left) reference experiment and (right) Exp3 during a convective situation at 1800 UTC 14 Aug 2021.

both radiosondes and GNSS dramatically decreases in the convective case (Fig. 16), while it slightly increases in the stratiform case (Fig. 17). This indicates that although the radar radial velocity may not have a direct effect on the moisture for example, the indirect effect can be big because of changes in the model balances.

In the convective case it can also be seen that the wind observations from other source than radar, synop, aircrafts (AIREP) and drifting buoys (DRIBU), have a higher impact when the radar radial velocities are added whereas in the stratiform case the effect on the other wind observations are small or even decrease.

b. Impact on the precipitation

In general, the precipitation is not affected very much when adding radar radial velocity to the observations used in the data assimilation. There are, however, a few situations where a positive impact can be seen.

One example, from 1800 UTC 26 August, is presented here. The radar image of 1-h accumulated precipitation valid at this time is shown in Fig. 18 (top). This image should be compared with the corresponding model output from a 6-h forecast (1-h accumulated precipitation) in Fig. 18 (bottom) with the reference run in the left panel and Exp3 in the right panel. The figures are zoomed in over the southern part of Sweden where the radar image has the most intense precipitation placed over land.

In the reference run, this precipitation is a bit too weak and placed over the sea. In Exp3, on the other hand, the intensity is higher and the area with the maximum intensity is placed over land, that is, much more similar to the radar image. In addition, the intense precipitation on the southern part of the island Öland, just east of the Swedish coast, is captured by Exp3 but almost totally missed in the reference case.

8. Discussion and conclusions

The assimilation of radar radial velocity data provided by the OPERA network was shown to improve the weather forecast skill in this study. These results were achieved by improving the first-guess check limits and tuning the observation error for this observation type. Furthermore, the sensitivity

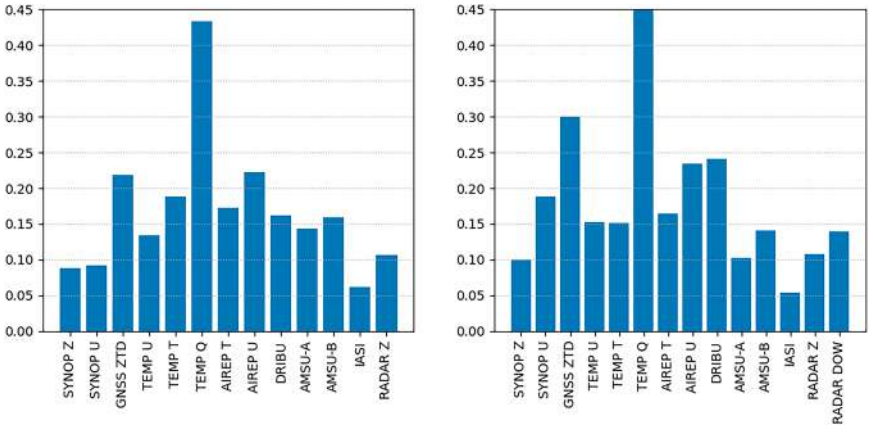

FIG. 17. As in Fig. 16, but during a situation with stratiform precipitation at 1800 UTC 17 Aug 2021.

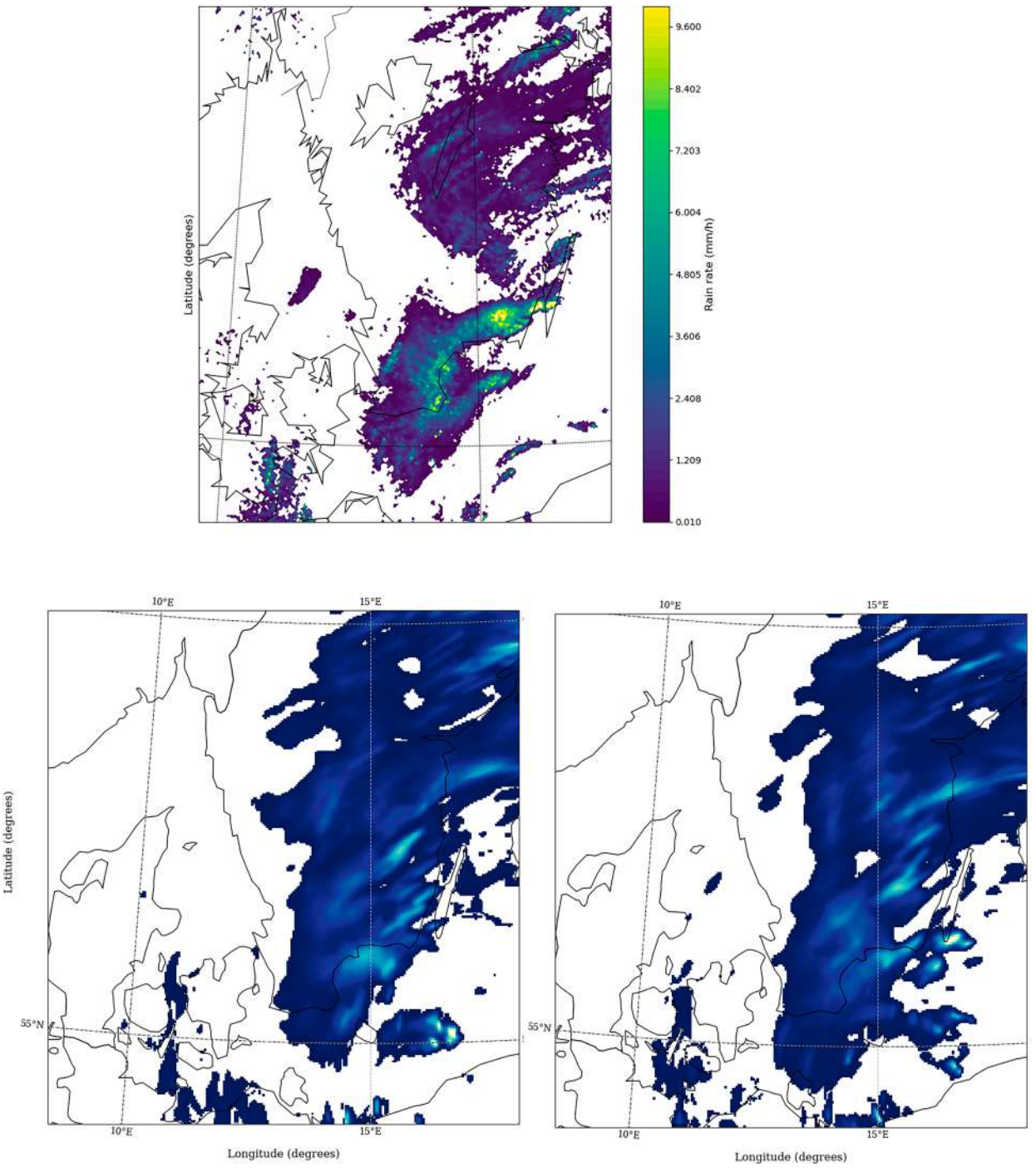

FIG. 18. (top) 1-h accumulated precipitation radar image, and 1-h accumulated model precipitation from (bottom left) the reference run and (bottom right) Exp3. All are valid at 1800 UTC 26 Aug 2021, and the model accumulations are between forecast lengths of 5 and 6 h. The color scale is the same in all panels.

between the skill scores and the size of the SO was briefly studied and a more beneficial size was found. Hence, we have shown that with proper preprocessing and harmonization of the radar radial velocity data, as well as the radar reflectivity data, provided by OPERA significant improvements are achievable. The impact of assimilating radar radial velocity has been studied over the MetCoop domain for a 1-month-long period in August 2021.

In this study it was found that the impact of the radar radial velocity observations can be improved by reducing the size of

the SOs. This will lead to more small-scale information being used and fewer data being averaged in the SO. The lower limit of the SO is decided by the memory capacity of the computer resource available since the main reason for reducing the number of radar data prior to the data assimilation is the capacity of the computer system.

Within the actual data assimilation system there is an additional reduction of the data amount. This depends on two things; the resolution of the model and the error correlations of the observations used. It was found here that instead of increasing the thinning distance to meet the observation error correlation lengths for radar radial velocity, the results improved when decreasing the thinning distance and at the same time increasing the observation error to compensate for any additional spatial correlation errors that may be introduced. This method could be applied to any high-resolution dataset, like Mode-S or crowdsource observations.

Moreover, it was shown that not only does the wind field improve when assimilating the radar radial velocity but also other parameters such as temperature and relative humidity close to the ground. It can also be seen by studying the DFS statistics that other observations, such as moisture from radiosondes and GNSS-ZTD, are better in balance and thereby the impact of these is improved as well. This is most pronounced during convective situations.

For case studies of precipitation events the effect of adding radial velocity was not very pronounced. This is natural since the precipitation is more sensitive to the reflectivity fields in the radar observations. However, a few cases where both the intensity and the position of the precipitation were improved were identified. The identification of these cases is very subjective, so a better, more objective way would be to use a spatial verification. A verification tool for this is under development but not available at the time of this study.

The most optimal settings as found in this paper will lead to an increased amount of data entering the assimilation system. This can cause problems with memory during the runs depending on the computer resources available. However, if run on such a system it is possible to assimilate the radar radial velocity with the same resolution as the radar reflectivity and still get good results. This was shown in the paper where experiment 1 represents such a scenario. The possible issues with memory can be even more severe when running four-dimensional variational (4Dvar) data assimilation in which the time dimension is also taken into account. This will be the natural next step in the radar data assimilation since a 4Dvar implementation is ongoing within the HARMONIE–AROME system.

After this study was completed, the radar radial velocities were included in operational MetCoOp production. The operational radar radial velocity assimilation uses the settings described in section 4 and in accordance with experiment 3 in section 5 in this paper, that is, smaller SO size for radial velocity as well as less thinning than radar reflectivity in the data assimilation. The operationalization followed after a long period in the preoperational suite. This indicates that the good results shown here also are valid for other periods and weather situations.

The methods described here are not specific for the HARMONIE–AROME system or radar radial velocity. They can be applied to any high-resolution observations in any data assimilation system. However, the specific settings need to be adjusted to fit with the model resolution as well as the observation type used in each case.

Acknowledgments. The authors thank Beatriz Navascués and Magnus Lindskog for good discussions about the use of data in the model and Gunther Haase for valuable advice and expertise on the radar observations.

Data availability statement. Datasets used in the paper are publicly available upon request.

REFERENCES

Anderson, E., and H. Järvinen, 1999: Variational quality control. *Quart. J. Roy. Meteor. Soc.*, **125**, 697–722, https://doi.org/10.1002/qj.49712555416.

Bengtsson, L., and Coauthors, 2017: The HARMONIE–AROME model configuration in the ALADIN–HIRLAM NWP system. *Mon. Wea. Rev.*, **145**, 1919–1935, https://doi.org/10.1175/MWR-D-16-0417.1.

Benjamin, S. G., 1989: An isentropic mesoα-scale analysis system and its sensitivity to aircraft and surface observations. *Mon. Wea. Rev.*, **117**, 1586–1603, https://doi.org/10.1175/1520-0493(1989)117<1586:AIMSAS>2.0.CO;2.

Bormann, N., and P. Bauer, 2010: Estimates of spatial and interchannel observation-error characteristics for current sounder radiances for numerical weather prediction. I: Methods and application to ATOVS data. *Quart. J. Roy. Meteor. Soc.*, **136**, 1036–1050, https://doi.org/10.1002/qj.616.

Caumont, O., and Coauthors, 2006: A radar simulator for high-resolution nonhydrostatic models. *J. Atmos. Oceanic Technol.*, **23**, 1049–1067, https://doi.org/10.1175/JTECH1905.1.

——, V. Ducrocq, É. Wattrelot, G. Jaubert, and S. Pradier-Vabre, 2010: 1D+3DVar assimilation of radar reflectivity data: A proof of concept. *Tellus*, **62A**, 173–187, https://doi.org/10.1111/j.1600-0870.2009.00430.x.

Chapnik, B., G. Desroziers, F. Rabier, and O. Talagrand, 2006: Diagnosis and tuning of observational error in a quasi-operational data assimilation setting. *Quart. J. Roy. Meteor. Soc.*, **132**, 543–565, https://doi.org/10.1256/qj.04.102.

Desroziers, G., L. Berre, B. Chapnik, and P. Poli, 2005: Diagnosis of observation, background and analysis-error statistics in observation space. *Quart. J. Roy. Meteor. Soc.*, **131**, 3385–3396, https://doi.org/10.1256/qj.05.108.

Frehlich, R., 2008: Atmospheric turbulence component of the innovation covariance. *Quart. J. Roy. Meteor. Soc.*, **134**, 931–940, https://doi.org/10.1002/qj.263.

Haase, G., and T. Landelius, 2004: Dealiasing of Doppler radar velocities using a torus mapping. *J. Atmos. Oceanic Technol.*, **21**, 1566–1573, https://doi.org/10.1175/1520-0426(2004)021<1566:DODRVU>2.0.CO;2.

Hagelin, S., R. Azad, M. Lindskog, H. Schyberg, and H. Körnich, 2021: Evaluating the use of Aeolus satellite observations in the regional numerical weather prediction (NWP) model Harmonie–Arome. *Atmos. Meas. Tech.*, **14**, 5925–5938, https://doi.org/10.5194/amt-14-5925-2021.

Hanssen, A. W., and W. J. A. Kuipers, 1965: *On the Relationship Between the Frequency of Rain and Various Meteorological Parameters.* KNMI Communications and Treatises, Vol. 81, Staatsdrukkerij- en Uitgeverijbedrijf, 86 pp.

He, G., J. Sun, Z. Ying, and L. Zhang, 2019: A radar radial velocity dealiasing algorithm for radar data assimilation and its evaluation with observations from multiple radar networks. *Remote Sens.*, **11**, 2457–2473, https://doi.org/10.3390/rs11202457.

Hollingsworth, A., 1989: The role of real-time four-dimensional data assimilation in the quality control, interpretation, and synthesis of climate data. *Oceanic Circulation Models: Combining Data and Dynamics*, D. L. T. Anderson and J. Willebrand, Eds., Springer, 303–343.

Huuskonen, A., E. Saltikoff, and I. Holleman, 2014: The operational weather radar network in Europe. *Bull. Amer. Meteor. Soc.*, **95**, 897–907, https://doi.org/10.1175/BAMS-D-12-00216.1.

Lindskog, M., H. Järvinen, and D. B. Michelson, 2000: Assimilation of radar radial winds in the HIRLAM 3D-Var. *Phys. Chem. Earth*, **25B**, 1243–1249, https://doi.org/10.1016/S1464-1909(00)00187-8.

——, K. Salonen, H. Järvinen, and D. B. Michelson, 2004: Doppler radar wind data assimilation with HIRLAM 3DVAR. *Mon. Wea. Rev.*, **132**, 1081–1092, https://doi.org/10.1175/1520-0493(2004)132<1081:DRWDAW>2.0.CO;2.

Liu, Z.-Q., and F. Rabier, 2003: The potential of high-density observations for numerical weather prediction: A study with simulated observations. *Quart. J. Roy. Meteor Soc.*, **129**, 3013–3035, https://doi.org/10.1256/qj.02.170.

Michelson, D., and A. Henja, 2012: Opera work package 3.6: Odyssey additions, task 3: Tuning and evaluation of "andre" tool. OPERA Tech. Rep. Working Doc. WD-2012-02c, 20 pp.

Montmerle, T., and C. Faccani, 2009: Mesoscale assimilation of radial velocities from Doppler radars in a preoperational framework. *Mon. Wea. Rev.*, **137**, 1939–1953, https://doi.org/10.1175/2008MWR2725.1.

Müller, M., and Coauthors, 2017: AROME-MetCoOp: A Nordic convective-scale operational weather prediction model. *Wea. Forecasting*, **32**, 609–627, https://doi.org/10.1175/WAF-D-16-0099.1.

Purser, R. J., D. Parrish, and M. Masutani, 2000: Meteorological observational data compression; an alternative to conventional "super-obbing." NCEP Office Note 430, 13 pp., http://www.emc.ncep.noaa.gov/mmb/papers/purser/on430.pdf.

Randriamampianina, R., T. Iversen, and A. Storto, 2011: Exploring the assimilation of IASI radiances in forecasting polar lows. *Quart. J. Roy. Meteor. Soc.*, **137**, 1700–1715, https://doi.org/10.1002/qj.838.

Ray, P. S., and C. Ziegler, 1977: De-aliasing first-moment Doppler estimates. *J. Appl. Meteor.*, **16**, 563–564, https://doi.org/10.1175/1520-0450(1977)016<0563:DAFMDE>2.0.CO;2.

Rennie, M. P., L. Isaksen, F. Weiler, J. de Kloe, T. Kanitz, and O. Reutebuch, 2021: The impact of Aeolus wind retrievals on ECMWF global weather forecasts. *Quart. J. Roy. Meteor. Soc.*, **147**, 3555–3586, https://doi.org/10.1002/qj.4142.

Ridal, M., and M. Dahlbom, 2017: Assimilation of multinational radar reflectivity data in a mesoscale model: A proof of concept. *J. Appl. Meteor. Climatol.*, **56**, 1739–1751, https://doi.org/10.1175/JAMC-D-16-0247.1.

Rihan, F. A., C. G. Collier, S. P. Ballard, and S. J. Swarbrick, 2008: Assimilation of Doppler radial winds into a 3D-Var system: Errors and impact of radial velocities on the variational analysis and model forecasts. *Quart. J. Roy. Meteor. Soc.*, **134**, 1701–1716, https://doi.org/10.1002/qj.326.

Salonen, K., H. Järvinen, S. Järvenoja, S. Niemelä, and R. Eresmaa, 2008: Doppler radar radial wind data in NWP model validation. *Meteor. Appl.*, **15**, 97–102, https://doi.org/10.1002/met.47.

——, ——, G. Haase, S. Niemelä, and R. Eresmaa, 2009: Doppler radar radial winds in HIRLAM. Part II: Optimizing the super-observation processing. *Tellus*, **61A**, 288–295, https://doi.org/10.1111/j.1600-0870.2008.00381.x.

Simonin, D., S. P. Ballard, and Z. Li, 2014: Doppler radar radial wind assimilation using an hourly cycling 3D-Var with a 1.5 km resolution version of the Met Office Unified Model for nowcasting. *Quart. J. Roy. Meteor. Soc.*, **140**, 2298–2314, https://doi.org/10.1002/qj.2298.

——, J. A. Waller, S. P. Ballard, S. L. Dance, and N. K. Nichols, 2019: A pragmatic strategy for implementing spatially correlated observation errors in an operational system: An application to Doppler radial winds. *Quart. J. Roy. Meteor. Soc.*, **145**, 2772–2790, https://doi.org/10.1002/qj.3592.

Sun, J., 2005: Convective-scale assimilation of radar data: Progress and challenges. *Quart. J. Roy. Meteor. Soc.*, **131**, 3439–3463, https://doi.org/10.1256/qj.05.149.

Wattrelot, E., O. Caumont, and J.-F. Mahfouf, 2014: Operational implementation of the 1D+3D-var assimilation method of radar reflectivity data in the AROME model. *Mon. Wea. Rev.*, **142**, 1852–1873, https://doi.org/10.1175/MWR-D-13-00230.1.

Xiao, Q., Y.-H. Kuo, J. Sun, W.-C. Lee, E. Lim, Y.-R. Guo, and D. M. Barker, 2005: Assimilation of Doppler radar observations with a regional 3DVAR system: Impact of Doppler velocities on forecasts of a heavy rainfall case. *J. Appl. Meteor.*, **44**, 768–788, https://doi.org/10.1175/JAM2248.1.